

Editorial revision 4/25/2013 4/25/2013 2:04:47 PM

1 **Revision 2**

2 **The origin of melanophlogite, a clathrate mineral, in natrocarbonatite lava at Oldoinyo**  
3 **Lengai, Tanzania.**

4

5 A.D.Beard<sup>1</sup>, K. Howard<sup>2</sup>, L. Carmody<sup>3</sup> and A.P.Jones<sup>3</sup>

6 1. Department of Earth and Planetary Sciences, Birkbeck, University of London, Malet  
7 Street, London, WC1E 7HX, UK.

8 2. Natural History Museum, Mineralogy Department, Cromwell Road, London SW7  
9 5BD, UK.

10 3. Department of Earth Sciences, University College London, Gower Street, London. WC1E  
11 6BT, UK.

12 Corresponding author ✉ [a.beard@ucl.ac.uk](mailto:a.beard@ucl.ac.uk)

13

14 **Abstract**

15 We report new observations of a clathrate mineral, melanophlogite  
16 ( $46\text{SiO}_2 \cdot 6(\text{N}_2, \text{CO}_2) \cdot 2(\text{CH}_4, \text{N}_2)$ ), as part of a tuffaceous layer within a sample of the 2006  
17 natrocarbonatite lava, whose composition reflects the typical magma erupted passively at  
18 Oldoinyo Lengai throughout the last ~50 years. The mineral has been identified by chemical  
19 composition, micro X-ray diffraction and transmitted light optical characteristics. This is the  
20 first reported occurrence of a clathrate in an igneous carbonatite, and we conjecture that this  
21 mineral may be recognized elsewhere in alteration products of natrocarbonatite ash and in  
22 particular, combeite-bearing carbonatite lithologies. Specifically, melanophlogite is a rare  
23 polymorph of  $\text{SiO}_2$  with guest molecules (e.g.  $\text{CH}_4$ ,  $\text{CO}_2$ ,  $\text{SO}_2$ ,  $\text{N}_2$ ,  $\text{OH}$ ,  $\text{Xe}$ , and  $\text{Kr}$ ) within a  
24 silicate framework. It occurs in an ash pellet-rich layer within the natrocarbonatite lava, as  
25 abundant groundmass crystals and as cores of individual ash pellets, with pseudocubic and  
26 pseudohexagonal habits, ranging from 50 to 100  $\mu\text{m}$  in size, with numerous inclusions of  
27 nepheline laths aligned parallel to the crystal margins. It has high C contents (up to 2.25  
28 wt.%) and  $\text{CO}_2$  is considered to be the guest molecule due to crystallisation within an alkaline  
29 carbonatitic- $\text{CO}_2$ -rich environment.

30

31 Keywords: Oldoinyo Lengai, melanophlogite, natrocarbonatite, combeite

32

33

34 **Introduction**

1

Editorial revision 4/25/2013 4/25/2013 2:04:47 PM

35 Oldoinyo Lengai (OL), situated in the Eastern Africa Rift Valley in NW Tanzania  
36 (Fig.1a), is the world's only active carbonatite volcano, forming a steep-sided stratocone  
37 rising to an altitude of 2960 m. Although OL is well-known for its unique natrocarbonatite  
38 lavas which have characterized activity since at least 1966, it is predominantly composed of  
39 nephelinitic and phonolitic lavas and pyroclastic deposits (Dawson, 1962, 1989, 1998). In this  
40 paper, we report the first occurrence of melanophlogite pseudomorphs after combeite,  
41 identified by electron microprobe (EMP) and confirmed by micro-Xray diffraction, from an  
42 ash pellet-rich layer within the March - April 2006 lava flows that occurred on the western  
43 flanks of OL. Melanophlogite is a very rare tetragonal (pseudocubic) polymorph of SiO<sub>2</sub> with  
44 structure-stabilising guest molecules (e.g. CH<sub>4</sub>, CO<sub>2</sub>, SO<sub>2</sub>, N<sub>2</sub>, OH, Xe, Kr) trapped within a  
45 clathrate-type silicate framework. This occurrence of melanophlogite is the first from Africa  
46 and the first from a carbonatite. The presence of broken melanophlogite pseudomorphs after  
47 combeite crystals requires that these pseudomorphs formed before the ash pellets were  
48 deposited. We present compositional and textural information in an attempt to understand its  
49 origin and significance at OL.

50

51

## 52 **Sample location**

53 The largest natrocarbonatite lava flow reported from OL occurred from March 25<sup>th</sup> and  
54 continued until April 5<sup>th</sup> 2006. The first effusive eruption on March 25<sup>th</sup> 2006 was associated  
55 with hornito collapse, overflowing of the summit crater, and emplacement of a 3 km long lava  
56 flow on the western flank (Kervyn et al., 2008). The lava tongue was initially confined to a  
57 deeply incised erosional gully, 15 - 20 m wide, before coming to a halt on the rift floor at an  
58 altitude of 1500 m and forming a distal lobe 150 m wide (Fig. 1b). A second effusive event  
59 occurred on April 3<sup>rd</sup> 2006, producing a flow passing through the same mid-slope gully on top  
60 of the cooled earlier lava flow (Kervyn et al., 2008). Flow morphologies are highly variable,  
61 changing considerably over a few meters, including scoriaceous, rubbly pahoehoe and blocky  
62 aa-type surfaces (Kervyn et al., 2008). The volume of lava produced during this eruptive  
63 event has been estimated at  $9.2 (\pm 3.0) \times 10^5 \text{ m}^3$ . During the period between the eruptions OL  
64 was continuously active, producing a large ash plume with ash fall observed over a wide area.  
65 In September 2007, three samples (OLD1-3) from the 2006 flows were collected from an  
66 altitude of 1850 m (Latitude 2°45'35"S; Longitude 35°53'43"E), by Mr. Colin Church.

67

## 68 **Analytical Methods**

2

Editorial revision 4/25/20134/25/2013 2:04:47 PM

69 A concentrated separate of melanophlogite crystals from the ash pellet layer was obtained by  
70 lightly crushing a subsample in a steel piston and sieving the crushed material into >850, 450  
71 and <450 $\mu\text{m}$  fractions. As melanophlogite does not react readily with dilute acid, the <450  
72  $\mu\text{m}$  fraction was washed in 10% HCl to remove carbonate and to concentrate the sample. It  
73 was then rinsed with distilled water to remove acid residues and dried under heat lamps. The  
74 acid-washed material was then subdivided using 250 and 63 $\mu\text{m}$  sieves. The melanophlogite  
75 crystals were mostly in the concentrated >63 $\mu\text{m}$  fraction and were then handpicked using fine  
76 acupuncture needles and prepared as polished grain mounts for SEM, EMPA and micro-Xray  
77 diffraction analysis.

78

79 Major element mineral analyses were obtained using a Jeol JXA8100 Superprobe (WDS) and  
80 an Oxford Instruments INCA system (EDS) at UCL/Birkbeck. Analysis was carried out using  
81 an accelerating voltage of 15 kV, current of  $2.5 \times 10^{-8}\text{A}$  and a beam diameter of 1 $\mu\text{m}$ . The  
82 counting times were 20s on the peak and 10s each on the high and low backgrounds.  
83 Analyses were calibrated against standards of natural silicates, oxides and Spec-pure metals  
84 with the data corrected using a ZAF program. Carbon was calibrated against a synthetic  
85 moissanite (SiC) standard, using a counting time of 10s on the peak and 5s each on the high  
86 and low backgrounds and a beam diameter of 5 $\mu\text{m}$ . Elemental line-scans across individual  
87 melanophogite grains were obtained using an accelerating voltage of 15 kV with an  
88 acquisition time of 240s and a beam current of  $1 \times 10^{-8}\text{A}$  with a diameter of 1 $\mu\text{m}$ . Although,  
89 samples were carbon coated to provide electric conductivity, it was assumed the contribution  
90 of the carbon coating would be the same for across the whole surface.

91

## 92 **Petrology of lavas**

93 In hand specimen, lava samples OLD1 and OLD2 are light-grey, fine- to medium-grained  
94 and slightly vesiculated. Sample OLD3 is dark-grey, fine- to medium-grained with pahoehoe-  
95 like flow features on its uppermost surface and contains a conspicuous layer (1-2 cms thick)  
96 of abundant well-rounded ash pellets up to 1-2 mm in diameter (Fig. 2) similar in size and  
97 appearance to ash erupted during September 2007 (Mitchell and Dawson, 2007; Mattsson and  
98 Reusser, 2010). Previous studies of natrocarbonatite lavas have reported rounded fine-grained  
99 silicate aggregates mantling a single silicate crystal referred to as “silicate spheroids”  
100 (Kervyn et al., 2008; Mattsson and Vuorinen, 2009). They have been considered as evidence  
101 of silicate-carbonate immiscibility (Dawson et al., 1994; Church and Jones, 1995). In this  
102 study such rounded structures in sample OLD3 are referred to as “ash pellets” and “cored ash

3

Editorial revision 4/25/2013 4/25/2013 2:04:47 PM

103 pellets”, according to the classification scheme of ash particles and accretionary lapilli  
104 proposed by Brown et al. (2010), while those in the natrocarbonatite lava samples OLD1 and  
105 OLD2 are referred to as “silicate spheroids”. A polished thin section was prepared through  
106 the ash layer of OLD3. Petrographical textures of samples OLD1 and OLD2 agree with  
107 published descriptions of the same lava flow (Kervyn et al., 2008; Mattsson and Vuorinen,  
108 2009). It is aphyric with a well-developed trachytic texture defined by subparallel alignment  
109 of microphenocrysts of nyerereite ( $(\text{Na}_2\text{Ca}(\text{CO}_3)_2)$ ) and rounded subhedral gregoryite  
110 ( $(\text{Na}_2, \text{K}_2, \text{Ca})\text{CO}_3$ ), up to 2- 4 mm in diameter. The gregoryite microphenocrysts are zoned  
111 with cores containing numerous rounded inclusions of nyerereite, surrounded by clear  
112 inclusion-free rims. The interstitial groundmass consists of fine-grained nyerereite and  
113 gregoryite in close association with a skeletal network of fluorite, manganian magnetite,  
114 galena, barite, manganian monticellite, alabandite (MnS), REE-silica-rich-apatite, strontian  
115 witherite, rare gold and an unnamed Ba-V-Sr O-rich mineral phase. Isolated single subhedral-  
116 to-euhedral crystals of diopside, nepheline, wollastonite and rounded cored silicate spheroids  
117 (up to 2mm in diameter) are also found within the natrocarbonatite (Fig. 3). No evidence of  
118 interaction between natrocarbonatite and the silicate matrix of the ash pellets was observed.  
119 The silicate spheroids consist of single subhedral-euhedral crystal cores of nepheline,  
120 wollastonite, diopside and rare sodalite, mantled by a fine-grained aggregate of nepheline,  
121 combeite, diopside, melilite, wollastonite, titanian garnet (andradite-schorlomite) and titanian  
122 magnetite in a groundmass of Sr-rich calcite. Significantly, the combeite grains in the fine-  
123 grained aggregate of the silicate spheroid, have rectangular and hexagonal outlines, reach 100  
124  $\mu\text{m}$  in diameter and contain inclusions of nepheline laths. Combeite is also present as well-  
125 developed replacement rims around wollastonite and clinopyroxene crystal cores (Fig. 4).

126  
127 The ash pellet layer in sample OLD3 is free of nyerereite and gregoryite but is dominated by  
128 abundant rounded ash pellets, cored ash pellets and silicate phenocrysts, ranging in size from  
129 3 to 0.5 mm. The phenocrysts are subhedral - euhedral and consist of nepheline, wollastonite,  
130 melilite, titanian garnet, clinopyroxene and rare titanite. The ash pellets consist of single  
131 euhedral-subhedral crystal cores of nepheline, wollastonite, melilite and melanophlogite after  
132 combeite, mantled by finer-grained nepheline, melilite, wollastonite, clinopyroxene, titanian  
133 garnet and titanian magnetite in a matrix of Sr-bearing calcite. Similar composite crystal  
134 aggregates also occur as thin mantles around larger phenocrysts. Fluorapatite, titanian  
135 magnetite, barite, galena and Sr-rich calcite are common as groundmass phases. However,  
136 unlike the silicate spheroids in the lava samples, combeite is absent and appears to have been

Editorial revision 4/25/20134/25/2013 2:04:47 PM

137 replaced by melanophlogite, which occur as single pseudocubic crystal cores of the ash  
138 pellets and as abundant single pseudocubic and pseudo-hexagonal crystals within the fine-  
139 grained groundmass (Fig. 5). The phenocryst assemblage of nepheline, titanian garnet,  
140 melilite and wollastonite indicates that the ash pellet layer was derived from a melilite-  
141 bearing combeite-wollastonite-nephelinite magma (CWM) consistent with the description of  
142 Kervyn et al. (2008).

143

#### 144 **Mineral chemistry**

##### 145 **Lava flow samples (OLD1 and OLD2)**

146 Electron microprobe analyses of selected mineral phases from the lava flow samples (OLD1  
147 and OLD2) and from the ash pellet layer (OLD3) are given in Tables 1 and 2, respectively.

148 Both alkali carbonates, nyerereite and gregoryite, are characterised by high Na<sub>2</sub>O contents  
149 (ca. 23.5 wt.% and 44 wt.%, respectively) and relatively high contents of various minor  
150 elements. The nyerereite has high K<sub>2</sub>O (6.7 - 7 wt.%) and CaO (ca. 24.8 wt.%), with  
151 subordinate SrO (2.1 - 2.3 wt.%), BaO (0.5 - 0.6 wt.%), SO<sub>3</sub> (1.0- 1.5 wt.%), P<sub>2</sub>O<sub>5</sub> (0.37 -  
152 0.63 wt.%) and Cl (0.16 wt.%). The gregoryite has high K<sub>2</sub>O (2.0 - 2.4 wt.%), P<sub>2</sub>O<sub>5</sub> (3.8 - 4  
153 wt.%) and CaO (6.3 - 6.8 wt.%) contents, with subordinate amounts of SrO (1.1 - 1.3 wt.%),  
154 BaO (ca. 0.2 wt.%), SO<sub>3</sub> (3.7 - 4.0 wt.%) and Cl (0.14 - 0.18 wt.%). These compositions are  
155 identical to those reported in previous studies from OL natrocarbonatite (Keller and Krafft,  
156 1990; Zaitsev et al., 2009). Manganian monticellite occurs as very small subhedral grains (5  
157 - 25 μm in diameter) finely dispersed within the groundmass of the lava flow samples. It  
158 contains relatively high MnO (ca. 11.5 wt.%) and has been reported from other recent  
159 natrocarbonatite lavas (Mitchell and Belton, 2004; Church and Jones, 1995). Magnetite  
160 occurs as an abundant interstitial groundmass phase containing significant amounts of MnO  
161 (12 - 13 wt.%) with subordinate amounts of TiO<sub>2</sub> (1.3 wt. %). An unknown Ba-V oxide  
162 occurs as an interstitial groundmass phase associated with manganian monticellite, nepheline  
163 and apatite needles, forming subhedral-euhedral diamond-shaped crystals, up to 10-15 μm in  
164 length. It has very high BaO and V<sub>2</sub>O<sub>5</sub> contents (63 wt.% and 21 wt.%, respectively) with  
165 minor SrO (3.3 wt.%), CaO (2.5 wt.%), Na<sub>2</sub>O (1.8 wt.%) and MgO (0.87 wt.%). The  
166 presence of this Ba-V-oxide finely dispersed in the natrocarbonatite samples, is consistent  
167 with elevated whole-rock Ba and V contents obtained from effusive lavas flows from the OL  
168 summit crater during continuous activity in 1988 (Keller and Krafft, 1990). Nepheline,  
169 wollastonite, garnet, melilite and clinopyroxene occur in the cores and mantles of the silicate  
170 spheroids within the natrocarbonatite lava. They have compositions identical to those present

5

Editorial revision 4/25/2013 4/25/2013 2:04:47 PM

171 in the ash pellet layer sample (OLD3). Combeite was only observed in the fine-grained  
172 mantle around cored ash pellets, where it forms pseudocubic and rarer pseudo-hexagonal  
173 euhedral crystals, and also occurs as replacement rims around wollastonite and clinopyroxene  
174 crystal cores. Combeite is essentially a Na and Ca silicate with minor Fe, Mn and Mg  
175 contents. The Na/(Na+Ca) ratio (0.54) reveals that the combeite replacement rims have  
176 excess Na compared to the ideal value (0.50) for combeite ( $\text{Na}_2\text{Ca}_2\text{Si}_3\text{O}_9$ ). Such excess Na is  
177 consistent with other combeite reported from silicate lavas/ash from Oldoinyo Lengai and has  
178 been attributed to crystallization from a  $\text{Na}_2\text{CO}_3$ -rich magma (Dawson, 1989). A single  
179 crystal of sodalite found in the core of a silicate spheroid, contains significant FeO (~3.2  
180 wt.%) and  $\text{K}_2\text{O}$  (~3.5 wt.%) comparable to sodalite reported in nephelinite lava from OL  
181 (Dawson and Hill, 1998; Peterson, 1989). Titanian magnetite (7 - 8 wt. %  $\text{TiO}_2$ ; 1 - 2 wt.%  
182 MnO) occurs as an abundant phase in the fine-grained silicate mantle around single crystal  
183 cores.

184

#### 185 **Ash pellet layer (OLD3)**

186 Nepheline in the ash pellet layer has variable FeO (0.6 - 1.5 wt. %) and  $\text{Na}(\text{Na}/\text{K}) = 0.77 -$   
187 0.79, similar to nepheline from peralkaline nephelinite at OL (Dawson, 1998) and to the  
188 September 2007 ash eruption (Mitchell and Dawson, 2007). The garnet has variable  $\text{TiO}_2$   
189 (10.8 - 16.1 wt. %) and FeO (20.3 - 23.6 wt. %) with a compositional range from titanian  
190 andradite to schorlomite, comparable to garnet from older nephelinite lavas (Dawson, 1998).  
191 Clinopyroxene occurs as subhedral to euhedral phenocrysts displaying reverse zoning with  
192 rounded, partially corroded green hedenbergitic cores with high FeO (14.8 - 16.9 wt.%) and  
193 low MgO (6.5 - 8.5 wt.%) mantled by colourless diopsidic rims (8.8 - 12.2 wt.% FeO; (9.4 -  
194 12.8 wt. % MgO) . Such zoned clinopyroxene is seen in older OL lavas including olivine  
195 melilitites (Keller et al., 2006) phonolites and nephelinites (Dawson et al., 1994; Dawson,  
196 1998) and has been attributed to magma chamber convection and new magma injection  
197 (Dawson 1998). Melilite exhibits a narrow compositional range, with high  $\text{Na}_2\text{O}$  (5.2 - 5.4  
198 wt. %),  $\text{Al}_2\text{O}_3$  (5.6 - 7.1 wt.%) and FeO (7.4 - 9.6 wt.%) and subordinate MgO (3.9 - 4.7 wt.  
199 %). This melilite composition is remarkably similar to alumoåkermanite, a new mineral  
200 member of the melilite group, proposed by Wiedenmann et al. (2009). Wollastonite contains  
201 very low FeO ( $\approx 1$  wt.%) and MnO ( $\approx 0.2$  wt.%) similar to compositions in OL peralkaline  
202 nephelinite lavas (Dawson, 1998) and in the September 2007 ash eruption (Mitchell and  
203 Dawson, 2007). The titanian magnetite has similar composition to that in the fine-grained ash  
204 pellets in lava samples, having high  $\text{TiO}_2$  content (ca. 8 - 9 wt.%) and lower MnO (ca. 1

6

Editorial revision 4/25/2013 4/25/2013 2:04:47 PM

205 wt.%).

206

207 The melanophlogite occurs as abundant single isolated groundmass crystals and as cores of  
208 individual ash pellets in the ash-rich layer in sample OLD3 (Figs. 5 and 6). The concentrated  
209 fractions of melanophlogite have predominant pseudocubic and subordinate pseudo-hexagonal  
210 habits (Fig.7), ranging from 50 to 100  $\mu\text{m}$  in size. In thin-section, the melanophlogite is  
211 colourless in plane-polarised light, and isotropic in crossed polars. Backscattered imaging  
212 reveals numerous inclusions of nepheline laths and rarer inclusions of melilite needles and  
213 euhedral-subhedral titanian magnetite. The nepheline is predominately euhedral, up to 10  $\mu\text{m}$   
214 in length, with the C-axis preferentially orientated parallel to the melanophlogite crystal  
215 boundaries (Fig. 8). The melanophlogite displays a well-developed concentric compositional  
216 zonation usually with the outer marginal zones appearing darker in backscattered mode due  
217 to a higher concentration of the carbon-bearing guest molecule in the melanophlogite  
218 structure (Fig. 8). However, occasionally some melanophlogite crystals have intermediate  
219 growth zones with higher concentrations of the carbon-bearing guest molecule. High  
220 resolution elemental X-ray mapping of individual melanophlogite crystals reveals that the  
221 zoning corresponds to zones of carbon enrichment, especially towards the crystal margins  
222 (Fig.9). A high resolution line-scan across a zoned melanophlogite (Fig.10) confirms that  
223 carbon content increases while silica and oxygen contents decrease. A line-scan of chlorine  
224 was included to act as a control to ensure that any increase in carbon content was not due to a  
225 contribution from the carbon/chlorine based epoxy resin (Fig.10). Electron microprobe  
226 analysis of the melanophlogite reveals major Si (42 wt.%), O (56 wt.%) and C (3 wt.%)  
227 (Table 3). This melanophlogite structure was confirmed by micro X-ray diffraction at the  
228 Natural History Museum, London. The presence of minor Ca, Al, Na and K in some crystals  
229 is attributed to the presence of nepheline micro-inclusions.

230

### 231 **Worldwide occurrence of melanophlogite**

232 Melanophlogite (ideal formula  $46\text{SiO}_2 \cdot 6(\text{N}_2, \text{CO}_2) \cdot 2(\text{CH}_4, \text{N}_2)$ ) is a rare tetragonal  
233 (pseudocubic) polymorph of  $\text{SiO}_2$  with guest molecules (e.g.  $\text{CH}_4$ ,  $\text{CO}_2$ ,  $\text{SO}_2$ ,  $\text{N}_2$ ,  $\text{Xe}$ ,  $\text{Kr}$ ,  $\text{OH}$ )  
234 entrained within a clathrate-type silicate framework (Skinner and Appleman, 1963). It has  
235 been reported in only nine locations worldwide, being first described by Von Lasaulx (1876)  
236 from sulphur deposits in Racalmuto and Lercara, near Palermo, (Sicily). Subsequent  
237 occurrences include: Chvaletice, (Czech Republic) from metamorphosed Fe-rich  
238 rhodochrosite layers (Zak, 1967, 1972), Korozluky (Czech Republic) from fissures in tertiary

7

Editorial revision 4/25/2013 4/25/2013 2:04:47 PM

239 volcanic rocks (Filippi, 2002), Fortullino, (Tuscany, Italy) from a serpentinite breccia  
240 (Grassellini and Orlandi, 1972), Mount Hamilton, (Santa Clara County, California) from  
241 metamorphosed serpentine veins cutting sedimentary rocks (Cooper and Dunning, 1972),  
242 Clear Creek (San Benito County, California) from a former mercury mine (Dunning and  
243 Cooper, 2002), Lombard, (Napa Country, California) from a disused dolomite quarry  
244 (Dunning and Cooper, 2002), Tsekur-Koyash, (Ukraine) from sulphur deposits (Kopasheva  
245 and Makarov, 1975) and Parma, (Northern Appennines, Italy) from interbedded marls and  
246 volcanoclastic sediments (Adorni and Tateo, 2004 and Adorni et al., 2007). Also a report of a  
247 dredged melanophlogite-bearing pebble recovered offshore from the Oregon Coast, Pacific  
248 Ocean, from a depth of 700 m, near a methane-rich vent (Kohler et al., 1999).

249

250 Melanophlogite from Sicily and Ukraine are dominated by sulphur with minor amounts of  
251 CO<sub>2</sub> and OH guest molecules, consistent with association with local sulphur deposits. In  
252 contrast, that from California, from the Northern Appennines and from the Czech Republic  
253 have a mixture of CO<sub>2</sub> and OH guest molecules, due to the association with local carbonate-  
254 rich country rocks (Table 3). The dredged melanophlogite-bearing pebble is reported to have  
255 CH<sub>4</sub> as the resident guest molecule attributed to proximity to a deep-sea methane-rich fluid  
256 producing vent (Kohler et al., 1999).

257

## 258 **Discussion**

259 Melanophlogite in the 2006 lava flow at OL is only the tenth reported worldwide, the first  
260 from Africa and the first to be recognised as replacement after combeite in natrocarbonatite.  
261 Although the presence of a guest carbon-rich molecule in the melanophlogite framework  
262 structure was indicated by EMPA, we have not unambiguously confirmed its true molecular  
263 nature. Nonetheless, the nature of the carbon-rich guest molecule is assumed to be CO<sub>2</sub>, by  
264 comparison with CO<sub>2</sub> in melanophlogite from other locations (Zak, 1972; Cooper and  
265 Dunning, 1972). In other words the melanophlogite in OL ash pellets is deemed to have  
266 significant CO<sub>2</sub> content (calculated 2.25 wt.% CO<sub>2</sub>) which we attribute to crystallisation  
267 within a carbonatite-rich environment, where CO<sub>2</sub> is expected to be freely available (Table  
268 3).

269

## 270 **Pseudomorphs after combeite**

271 Fresh combeite was observed only within silicate spheroids in natrocarbonatite lava samples  
272 (OLD1 and OLD2), where combeite crystals share distinctive textural similarity to

8



Editorial revision 4/25/2013 4/25/2013 2:04:47 PM

273 melanophlogite. In specimen OLD3, they have pseudocubic and pseudo-hexagonal outlines,  
274 an identical size range 80-100  $\mu\text{m}$  and contain numerous inclusions of nepheline laths. The  
275 associated mineralogy from silicate spheroids is also identical to the mineralogy of the ash  
276 sample (OLD3) which strongly suggests that they were both derived from very similar alkali-  
277 silicate magmas. We therefore interpret melanophlogite as a pseudomorph after combeite  
278 which is inferred to have been formerly present in the ash (OLD3). In detail, the presence of  
279 broken melanophlogite crystals (Fig. 5) requires that this alteration process occurred before  
280 the incorporation of the ash layer by 2006 lava.

281

### 282 **Misidentification of melanophlogite in previous studies.**

283 This study documents the first occurrence of melanophlogite from Oldoinyo Lengai.  
284 However, close reinspection of the literature suggests that melanophlogite may previously  
285 have been observed but not recognized, or misidentified. Hay (1989) reported an initially  
286 unidentified Na-Ca silicate mineral from the Laetoli Footprint Tuff and the nephelinite-  
287 carbonatite ash erupted in 1966, which was subsequently identified as combeite.  
288 Significantly, we note that some published combeite has been described as cubic and  
289 hexagonal grains, up to 100  $\mu\text{m}$  in size, with low birefringence, concentric zoning parallel to  
290 crystal faces and containing numerous inclusions of nepheline laths (Hay, 1989). This  
291 textural description is very similar to melanophlogite in the ash pellet layer from OLD3.  
292 However, Hay (1989) also observed that some of the combeite in both the Laetoli Footprint  
293 Tuff and the 1966 ash was partly or wholly altered to an unknown mineral phase with a  
294 composition similar to "opal". We conjecture that some of the alteration products observed  
295 in Hay's (1989) study are combeite partially pseudomorphed by melanophlogite. A second  
296 example was apparently reported by Dawson (1998) in wollastonite nephelinite lavas  
297 extruded from OL in 1993. A euhedral zoned combeite phenocryst, 100  $\mu\text{m}$  in size, with  
298 numerous inclusions of nepheline laths, was described with partial replacement by an  
299 unidentified alteration product enriched in Si ( $\text{SiO}_2$  79 wt.%), depleted in Ca and Na and with  
300 low analytical totals (Table 3). Dawson (1998) conjectured that the low totals for this  
301 alteration product may be due to unanalyzed elements like O, H or C. Again the low total,  
302 analysed composition and textural description is remarkably similar to microprobe analyses  
303 of melanophlogite reported in our study. A photomicrograph of the partially replaced  
304 combeite phenocryst in Dawson's 1998 paper appears to confirm the similarity to  
305 melanophlogite. Dawson (1998) also noted that the alteration of combeite enhanced  
306 symmetrical and concentric zoning, referring to the process of "skeletonization" proposed by

9

Editorial revision 4/25/20134/25/2013 2:04:47 PM

307 Bailey (1941) whereby the original crystals have been selectively leached of Ca, K and Na,  
308 without destroying the internal silica framework of the crystals. It seems likely that this  
309 “skeletonization” process refers to the secondary replacement of combeite by  
310 melanophlogite. The process of “skeletonization” could be attributed to be the secondary  
311 reaction replacing combeite with melanophlogite in the ash pellet layer. In this process, Ca,  
312 Na and K are selectively removed by leaching, from combeite, accompanied by increase in Si  
313 content. Bailey (1941) suggested that this process of “skeletonization” could be achieved by  
314 the presence of a leaching agent such as a weak acid.

315

316 Within the ash pellet-rich layer in sample OLD3, any combeite grains have been replaced by  
317 melanophlogite, suggesting that the alteration process occurred before the ash pellets were  
318 deposited on the lava surface. This is consistent with the recognition of broken  
319 melanophlogite grains occasionally present as cores of ash pellets indicating that pre-existing  
320 combeite pseudomorphs were entrained in the eruption prior to deposition of the ash layer.  
321 However, contemporaneous silicate spheroids within the natrocarbonatite, retain fresh  
322 combeite both as microphenocrysts and as replacement rims around clinopyroxene, indicating  
323 that combeite was only locally replaced by melanophlogite, and may instead constitute  
324 reworking of previous volcanic lithic materials.

325

326

### 327 **Conclusions**

328 We have documented the clathrate mineral melanophlogite as part of a tuffaceous layer  
329 within a sample of 2006 natrocarbonatite lava, whose composition reflects the “normal”  
330 magma type erupted nearly continuously at OL throughout the last ~50 years. The mineral  
331 has been characterised by chemical composition, transmitted light optical characteristics and  
332 *in-situ* micro X-ray diffraction. This is the first reported occurrence of a clathrate in a  
333 carbonatite, and is locally common. We conjecture that earlier descriptions refer to the same  
334 mineral in other carbonatite products from OL, and in regional descriptions of carbonatitic  
335 ash from the East African Rift. Therefore we can expect the occurrence of this mineral to be  
336 recognized elsewhere in alteration products of natrocarbonatite ash and in particular,  
337 combeite-bearing carbonatite lithologies. Future experiments to delineate the P-T stability of  
338 this clathrate could provide important constraints on the petrogenesis of natrocarbonatite, and  
339 add to the growing complexity of mineral pathways involved in rapid chemical weathering  
340 and distribution of alkaline salts in N Tanzania related to Lake Natron (Genge et al. 2001).

10

Editorial revision 4/25/2013 4/25/2013 2:04:47 PM

341

342 **Acknowledgements**

343 The authors are indebted to Mr. Colin E. Church for collecting the samples from the 2006  
344 natrocarbonatite lava flow and also to Abigail Church and James Robertson Safaris (Nairobi)  
345 for providing rock samples from the summit of Oldoinyo Lengai.

346

347

348 **References**

- 349 Adorni, F., Tateo, F., and Adorni, B. (2004) La melanophlogite di Case Montanini (S.  
350 Andrea B., Medesano), Appennino Parmense. *Rivista Mineralogica Italiana*, 3, 126 -  
351 136.
- 352 Adorni, F. and Tateo, F. (2007) A new melanophlogite occurrence from the Case  
353 Montanini Quarry, Parma, Northern Appennines, Italy. *Axis*, 3, 1 - 11.
- 354 Bailey, E.B. (1941) Skeletonized apophyllite from Crestmore and Riverside, California.  
355 *American Mineralogist*, 21, 565-566.
- 356 Brown, R.J., Branney, M.J., Maher, C., and Davila-Harris, P. (2010) Origin of accretionary  
357 lapilli within ground-hugging density currents: Evidence from pyroclastic couplets on  
358 Tenerife. *GSA Bulletin*, 122, 305-320.
- 359 Church, A. A. and Jones, A.P. (1995) Silicate-carbonate immiscibility at Oldoinyo Lengai.  
360 *Journal of Petrology*, 36, 869-889.
- 361 Cooper, J.F. and Dunning, G.E. (1972) Melanophlogite from Mount Hamilton, Santa Clara  
362 County, California. *American Mineralogist*, 57, 245 - 256.
- 363 Dawson, J.B. (1962) The geology of Oldoinyo Lengai. *Bulletin of Volcanology*, 24, 348 -  
364 387.
- 365 Dawson, J.B. (1989) Sodium carbonate lavas from Oldoinyo Lengai, Tanzania;  
366 implications for carbonatite complex genesis. In: K. Bell, Ed., *Carbonatites - Genesis*  
367 *and evolution*. Unwin Hyman, London, 255 - 277.
- 368 Dawson, J.B. (1998) Peralkaline nephelinite - natrocarbonatite relationships at Oldoinyo  
369 Lengai, Tanzania. *Journal of Petrology*, 39, 2077 - 2094.
- 370 Dawson, J.B., Pinkerton, H., Pyle, D. M., and Nyamweru, C. (1994) June 1993 eruption of  
371 Oldoinyo Lengai, Tanzania: Exceptionally viscous and large carbonatite lava flows and  
372 evidence for coexisting silicate and carbonate magmas. *Geology*, 22, 799 - 802.
- 373 Dawson, J.B. and Hill, P.G. (1998) Mineral chemistry of a peralkaline combeite  
374 lamprophyllite nepheline from Oldoinyo Lengai, Tanzania. *Mineralogical Magazine*, 62, 179

11

Editorial revision 4/25/2013 4/25/2013 2:04:47 PM

- 375 - 196.
- 376 Dunning, G.E. and Cooper, J.F. (2002) Pseudomorphic melanophlogites from California.  
377 Mineralogical Record, 33, 237-242.
- 378 Filippi, M. (2002) Melanoflogit – vzácný polymorf hmoty SiO<sub>2</sub> a jeho druhý výskyt v České  
379 republice. Bulletin Mineralogicko-petrografického oddělení Národního muzea v Praze, 10,  
380 120-130 (in Czech).
- 381 Genge, M. J., Balme, M., and Jones, A.P. (2001) Salt-bearing fumarole deposits in the  
382 summit crater of Oldoinyo Lengai: interactions between natrocarbonatite lava and meteoric  
383 water. Journal of Volcanology and Geothermal Research, 106, 111-122.
- 384 Grassellini, T.M. and Orlandi, P. (1972) Sulla melanoflogite del Fortullino (Livorno). Atti  
385 Soc. Tosc. Sc. Nat. Mem. Sr.A, 79, 245-250 (in Italian).
- 386 Hay, R. (1989) Holocene carbonatite-nephelinite tephra deposits of Oldoinyo Lengai,  
387 Tanzania. Journal of Volcanology and Geothermal Research, 37, 77 - 91.
- 388 Keller, J. and Krafft, M. (1990) Effusive natrocarbonatite activity of Oldoinyo Lengai,  
389 June, 1988. Bulletin of Volcanology, 52, 629 - 645.
- 390 Keller, J., Zaitsev, A., and Wiedenmann, D. (2006) Primary magmas at Oldoinyo Lengai; the  
391 role of olivine melilitites. Lithos, 91, 150-172.
- 392 Kervyn, M., Ernst, G.G.J., Klaudius, J., Keller, J., Kervyn, F., Mattsson, H.B., Belton, F.,  
393 Mbede, E., and Jacobs, P. (2008) Voluminous flows at Oldoinyo Lengai in 2006:  
394 chronology of events and insights into the shallow magmatic system. Bulletin of  
395 Volcanology, 70, 1069 - 1086.
- 396 Kohler, S., Irmer, G., Kleeberger Monecke, J., Herzig, P.M., and Schulz, B. (1999)  
397 Melanophlogite from the Cascadia accretionary prism, offshore Oregon: First occurrence  
398 from an active submarine vent site. European Journal of Mineralogy, 11, 129.
- 399 Kopasheva, S.K. and Makarov, J.J. (1975) First occurrence of melanophlogite in the  
400 USSR. Doklady Akademia Nauk, 224, 905 - 908 (in Russian).
- 401 Mattsson, H. B. and Vuorinen, J. (2009) Emplacement and inflation of natrocarbonatitic  
402 lava flows during the March-April 2006 eruption of Oldoinyo Lengai, Tanzania. Bulletin of  
403 Volcanology, 71, 301-311.
- 404 Mattsson, H. B. and Reusser, E. (2010) Mineralogical and geochemical characterization of  
405 ashes from an early phase of the explosive September 2007 eruption of Oldoinyo Lengai  
406 (Tanzania). Journal of African Earth Sciences, 58, 752-763.
- 407 Mitchell, R.H. and Belton, F. (2004) Niocalite-cuspidine solid solution and manganoan  
408 monticellite from natrocarbonatite, Oldoinyo Lengai, Tanzania. Mineralogical Magazine, 68,

12

Editorial revision 4/25/2013 4/25/2013 2:04:47 PM

- 409 787-799.
- 410 Mitchell, R.H. and Dawson, J.B. (2007) The 24<sup>th</sup> September 2007 ash eruption of the  
411 carbonatite volcano Oldoinyo Lengai, Tanzania: mineralogy of the ash and implication  
412 for the formation of a new hybrid magma type. *Mineralogical Magazine*, 75, 483 - 492.
- 413 Peterson, T.D. (1989) Peralkaline nephelinites: Comparative petrology of Shombole and  
414 Oldoinyo L'engai, East Africa. *Contributions to Mineralogy and Petrology*, 101, 458 - 478.
- 415 Skinner, B.J. and Appleman, D.E. (1963) Melanophlogite, a cubic polymorph of silica.  
416 *American Mineralogist*, 48, 854 - 867.
- 417 Von Lasaulx, A. (1876) *Mineralogisch-kristallographische Notizen*, VII. Melanophlogite  
418 ein neues mineral. *Neues Jahrbuch für Mineralogie*, 250 - 257.
- 419 Wiedenmann, D., Zaitsev, A.N., Britvin, S.N., Krivovichev, S.V., and Keller, J. (2009)  
420 Alumoåkermanite,  $(Ca,Na)_2(Al,Mg,Fe^{2+})(Si_2O_7)$ , a new mineral from the active  
421 carbonatite-nephelinite-phonolite volcano Oldoinyo Lengai, northern Tanzania.  
422 *Mineralogical Magazine*, 73, 373 - 384.
- 423 Zaitsev, A.N., Keller, J., Spratt, J., Jeffries, T., and Sharygin, V.V. (2009) Chemical  
424 composition of nyerereite and gregoryite from natrocarbonatite of Oldoinyo Lengai  
425 volcano, Tanzania. *Geology of Ore Deposits*, 51, 608 - 616.
- 426 Zak, L. (1967) Find of pyrophanite and melanophlogite in Chvaletice (E. Bohemia). *Časopis*  
427 *pro mineralogii a geologii*. 12, 451 - 452.
- 428 Zak, L. (1972) A contribution to the crystal chemistry of melanophlogite. *American*  
429 *Mineralogist*, 57, 779 - 796.
- 430
- 431
- 432 List of Figures
- 433 Figure. 1. Schematic maps showing the a) location of Oldoinyo Lengai within the East  
434 African Rift, Northern Tanzania. b) sample location on the main lava flow on the western  
435 flank of Oldoinyo Lengai (modified from Kervyn et al., 2008).
- 436 Figure 2. The ash pellet-rich layer in sample OLD3 consisting of well-rounded ash pellets,  
437 up to 1mm in diameter, deposited on a upper surface a cooled lava flow and subsequently  
438 covered by a later lava flow.
- 439 Figure 3. Backscattered electron image (BSE) of the April 2006 natrocarbonatite lava  
440 (OLD1) with lath-shaped nyerereite (ny) and sub-rounded gregoryite (gr) with a rare silicate  
441 spheroid (ss).

Editorial revision 4/25/20134/25/2013 2:04:47 PM

- 442 Figure 4. BSE image of a combeite replacement rim (com) around a wollastonite crystal  
443 (woll) in a silicate spheroid within the natrocarbonatite lava (OLD1).
- 444 Figure 5. BSE image of melanophlogite crystal cores of ash pellets and abundant single  
445 crystals, some revealing a broken appearance in the groundmass of the ash-pellet rich layer in  
446 OLD3. Abbreviations; mel=melanophlogite, neph=nepheline, ga= garnet, and  
447 woll=wollastonite.
- 448 Figure 6. A photomicrograph of an ash pellet with a melanophlogite core displaying well -  
449 developed concentric zoning. PPL. Abbreviations; mel=melanophlogite.
- 450 Figure 7. BSE image of melanophlogite revealing both pseudocubic and pseudo-hexagonal  
451 outlines. Abbreviations; mel=melanophlogite.
- 452 Figure 8. BSE image of melanophlogite displaying well-developed concentric  
453 zoning with a darker C-richer rim and including numerous inclusions of subhedral  
454 nepheline laths (light grey).
- 455 Figure. 9. X-ray elemental distribution maps of a melanophlogite crystal revealing  
456 concentric zonation, with increased carbon-rich zones towards crystal boundaries. Image  
457 labeled CP is a BSE reference image (grey scale).
- 458 Figure 10. EDS elemental linescan for C, O, Si and Cl across a zoned melanophlogite  
459 revealing increased carbon content.
- 460
- 461 Tables
- 462 Table 1. A summary of electron microprobe analysis for selective major mineral phases in  
463 the natrocarbonatite lava samples (OLD 1 and OLD2) and the silicate spheroids
- 464 Table 2. A selected summary electron microprobe analysis for selective major mineral phases  
465 in the ash pellet-rich layer (OLD3).
- 466 Table 3. Electron microprobe data for melanophlogite from the ash pellet-rich layer  
467 (OLD3) compared with melanophlogites from Sicily, Italy (Von Lasaulx, 1876), Czech  
468 Republic (Zak, 1967), California, U.S.A (Cooper and Dunning, 1972) and a  
469 partially replaced combeite, Oldoinyo Lengai (Dawson, 1998).

Table 1. Electron microprobe data for major mineral phases in the natrocarbonate lava samples (OLD 1 and OLD2) and the silicate spheroids.

Natrocarbonatite					Selected phases in natrocarbonatite groundmass								Selected silicate/oxide phases in the silicate spheroids											
Nyerereite		Gregoryite			Mn-Mag	Unknown	Ba-V-oxide		Silico-REE	Manganoan		monticellite	Combeite	Combeite	Combeite	Combeite	Neph	Woll	Mel	Garnet	Cpx	Soda	Ti-mag	
								apatite					gm	gm	rim-woll	rim-woll								
Na2O	23.64	23.52	43.29	44.24	SiO2	0.68	0	SiO2	8.54	SiO2	34.91	34.86	SiO2	50.26	50.04	50.47	51.69	42.11	51.43	43.32	29.98	51.39	35.41	0.33
P2O5	0.63	0.37	3.84	4.04	TiO2	1.34	0	TiO2	0.00	FeO	3.66	4.21	TiO2	0.36	0.08	0.00	0.00	0.00	0.29	0.59	13.73	0.42	0	7.62
SO3	1.53	1.02	3.75	3.96	Al2O3	0.77	0	Al2O3	0.10	MnO	11.55	11.38	Al2O3	0	0	0.14	0.40	31.98	0.00	6.75	0.68	0.82	27.07	0.19
K2O	6.79	7.09	2.39	2.02	FeO	75.88	0.8	FeO	0.15	MgO	15.20	15.02	FeO	0.20	0.06	0.14	0.17	1.98	1.33	6.69	21.87	13.82	3.21	74.34
CaO	24.89	24.76	6.33	6.79	MnO	12.60	0	MnO	0.00	CaO	33.98	33.74	MnO	0.37	0.27	0.39	0.01	0.02	0.55	0.78	0.44	0.51	0.13	1.83
MnO	0.10	0.09	0.12	0.10	Cr2O3	0.03	0	CaO	40.12				Cr2O3	0.41	0	0.19	0.33	0	0	0	0.17	0.13	0	0.06
SrO	2.18	2.29	1.36	1.16	V2O5	n.a	20.91	MgO	0.02	Total	99.30	99.20	MgO	0.55	0.51	0.44	0.48	0.15	0.10	4.5	0.51	9.37	0.17	2.36
BaO	0.54	0.65	0.23	0.19	CaO	1.05	2.48	Na2O	0.73				CaO	27.14	27.91	28.84	28.55	0.14	46.04	30.58	32.12	21.4	0	0.93
Cl	0.16	0.17	0.14	0.18	MgO	1.64	0.87	K2O	0.50				Na2O	19.46	19.72	18.74	18.27	15.09	0.13	4.97	0	2.37	21.68	0
					Na2O	0	1.79	SrO	3.57				K2O	0.09	0.17	0.43	0.13	7.68	0	0.1	0	0	3.5	0
Total	60.46	59.96	61.44	62.68	K2O	0	0.85	P2O5	27.95				P2O5	0.59	0.76	0.28	0.00	n.a	n.a	n.a	n.a	n.a	n.a	n.a
					BaO	n.a	63.03	La2O3	6.10				SO3	n.a	n.a	n.a	n.a	n.a	n.a	n.a	n.a	n.a	1.7	n.a
					SrO	n.a	3.3	Ce2O3	8.42				Cl	n.a	n.a	n.a	n.a	n.a	n.a	n.a	n.a	n.a	6.09	n.a
					SO3	n.a	1.17	SO3	0.12				Total	99.42	99.51	100.07	100.03	99.13	99.87	98.28	99.50	100.23	98.96	87.65
					Cl	n.a	3.33	F	0.75															
								Cl	0.55															
					Total	93.99	98.53	O=F,Cl	0.44				Na/(Na+Ca)	0.54	0.54	0.53	0.52							
								Total	97.18															

Abbreviations: n.a. = not analysed, gm=groundmass, Woll = wollastonite, neph = nepheline, Mel= melilite, mag= magnetite, soda = sodalite, Cpx= clinopyroxene, Ti-mag= titanian magnetite.

Table 2. Electron microprobe data for major mineral phases in the ash pellet-rich layer (OLD3).

	Nepheline				Garnet			Mellilite				Clinopyroxene					Wollastonite, titanite, apatite, magnetite							
	1	2	3	4	1	2	3	1	2	3	4	core 1	rim 1	core 2	rim2	Inclusion	Woll	Woll	Titanite	Apatite	Magnetite			
SiO2	43.71	43.31	43.46	43.03	28.92	28.98	31.97	43.65	44.13	43.83	43.41	52.34	52.87	52	50.97	51.52	SiO2	50.97	51.23	30.79	0.60	0.05		
TiO2	0	0	0	0	16.11	15.56	10.82	0.02	0.01	0.01	0.05	0.52	0.6	0.39	1.34	0.45	TiO2	0.04	0.06	38.35	0.00	8.46		
Al2O3	31.90	31.50	32.45	33.76	0.79	0.64	0.48	7.09	6.76	6.19	5.58	0.94	0.88	0.83	2.89	2.06	Al2O3	0.00	0.03	0.39	0.01	0.68		
FeO	1.28	0.62	1.54	1.29	20.35	21.09	23.57	7.4	7.4	9.5	9.64	14.88	12.21	16.9	8.89	13.01	FeO	1.04	0.99	1.35	0.09	84.11		
MnO	0.05	0.24	0.01	0.00	0.36	0.32	0.50	0.2	0.23	0.26	0.32	0.52	0.43	0.56	0.22	0.48	MnO	0.43	0.43	0.1	0.01	1.11		
MgO	0.04	0	0.00	0.10	0.92	1.08	0.32	3.96	4.7	4.28	4.64	7.71	9.42	6.5	12.82	9.3	MgO	0.17	0.14	0	0.01	0.48		
CaO	0.35	0.20	0.18	0.19	31.56	31.61	31.62	30.36	30.81	29.66	29.94	20.65	21.9	19.82	22.16	21.47	CaO	47.15	47.11	28.54	56.47	0.49		
Na2O	15.47	16.68	15.82	15.10	0.48	0.34	0.48	5.39	5.36	5.39	5.3	2.13	1.57	2.55	1.07	1.63	Na2O	0.04	0.05	0.1	0.01	0.05		
K2O	6.84	6.85	6.48	6.58	0	0	0	0.09	0.09	0.14	0.17	0	0	0	0	0	K2O	0.01	0.00	0	0.07	0.03		
Total	99.64	99.40	99.94	100.06	99.49	99.62	99.77	98.17	99.49	99.26	99.06	99.69	99.88	99.55	100.36	99.92	P2O5	n.a	n.a	n.a	40.96	n.a		
Na=(Na/K)	0.77	0.79	0.79	0.78	Py	2.12	2.47	0.76	mg#	48.86	53.08	44.55	46.17	0.52	0.58	0.47	0.8	0.63	F	n.a	n.a	n.a	1.74	n.a
					And	26.33	27.1	31.46									Cl	n.a	n.a	n.a	0.01	n.a		
					Scho	18.75	17.98	12.99									Total	99.84	100.05	99.62	99.96	95.45		
					Gro	52.31	52.08	54.07																
					Sp	0.47	0.42	0.68																
					Uv	0.02	0	0.04																

Abbreviations: n.a. = not analysed, Woll = wollastonite, Py = pyrope, And= andradite, Scho=schorlomite, Gro= grossular, Sp=spessartine, Uv= Uvarovite, mg#= Mg/(Mg+Fe<sup>2+</sup>).



Table 3. Electron microprobe data for melanophlogite from the ash pellet-rich layer (OLD3) compared with melanophlogites from Sicily, Italy (Von Lasaulx, 1876), The Czech Republic (Zak, 1967), California, U.S.A (Cooper and Dunning, 1972) and a partially replaced combeite, Oldoinyo Lengai (Dawson, 1998).

	n=10 Oldoinyo Lengai Tanzania	Racalmuto Sicily Italy	Chvaletice The Czech Republic	Mt. Hamilton California U.S.A	Partially replaced combeite (from Dawson, 1998)	
wt. %						
Si	41.35	43.21	44.23	44.97	Si	36.51
S	n.d	2.28	0.1	0.01	S	0
O	55.9	52.61	52.97	53.44	O	45.36
C	2.25	1.2	0.9	0.84	Fe	1.13
H	n.a	0.81	0.6	0.79	Mg	1.27
					Ca	3.5
Total	99.5	100.11	98.8	100.05	Na	0.29
					K	0.59
					Total	88.65

Abbreviations: n.d = not detected; n.a.= not analysed.

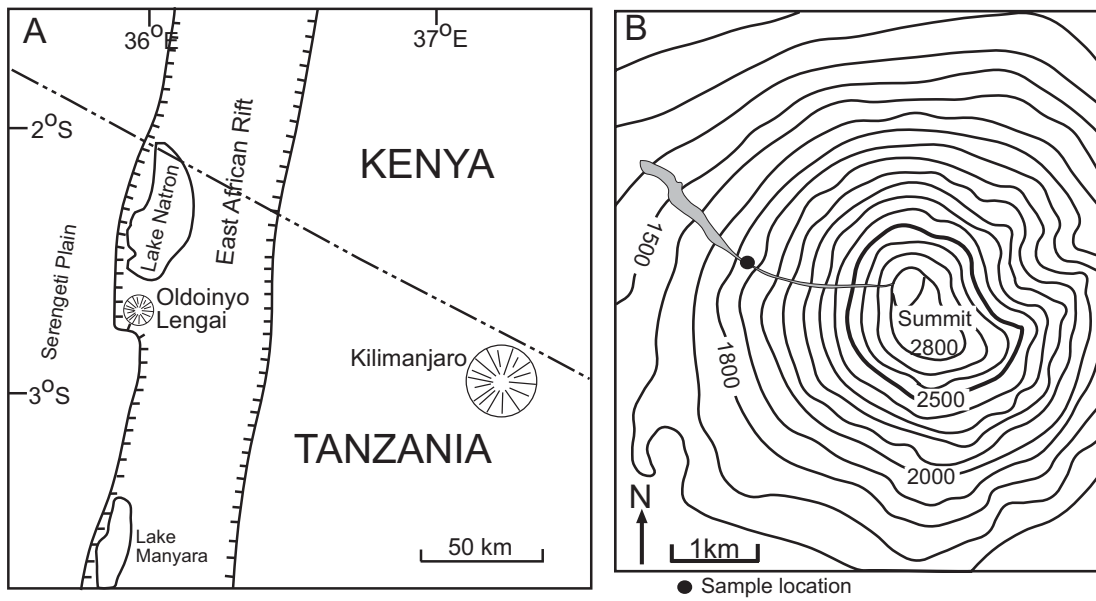


Figure 1



Figure 2

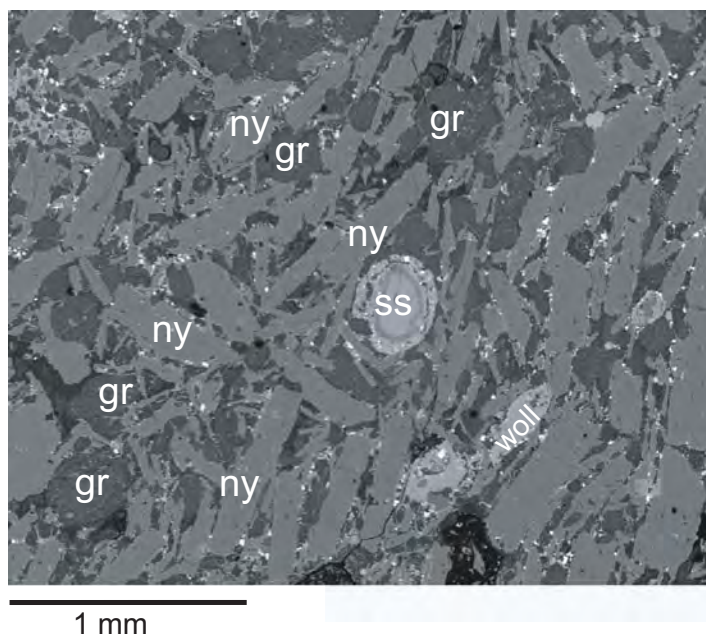


Figure 3

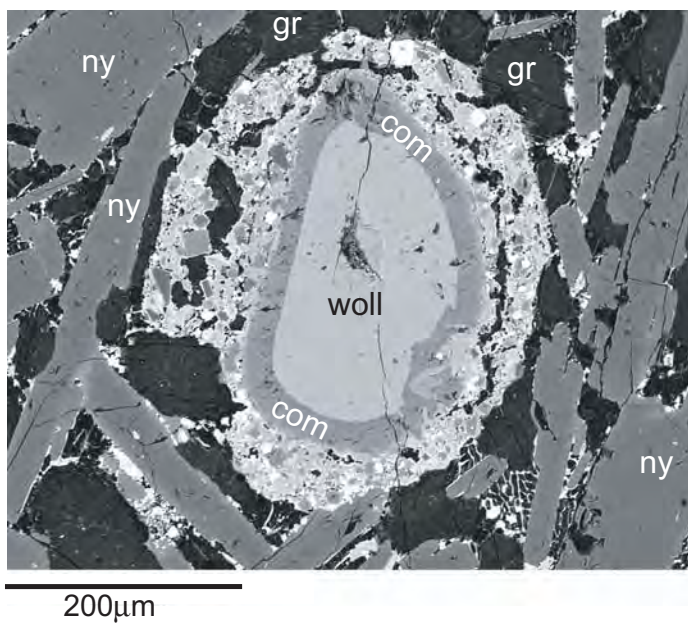


Figure 4

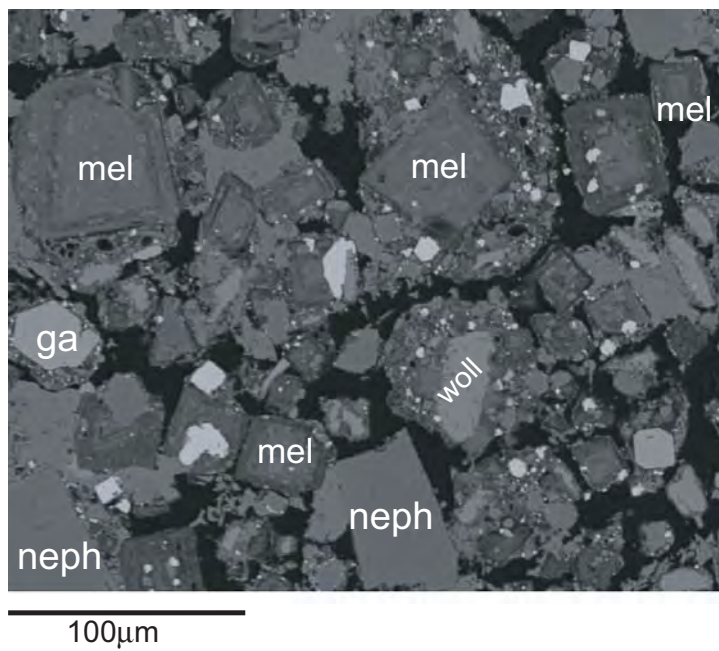
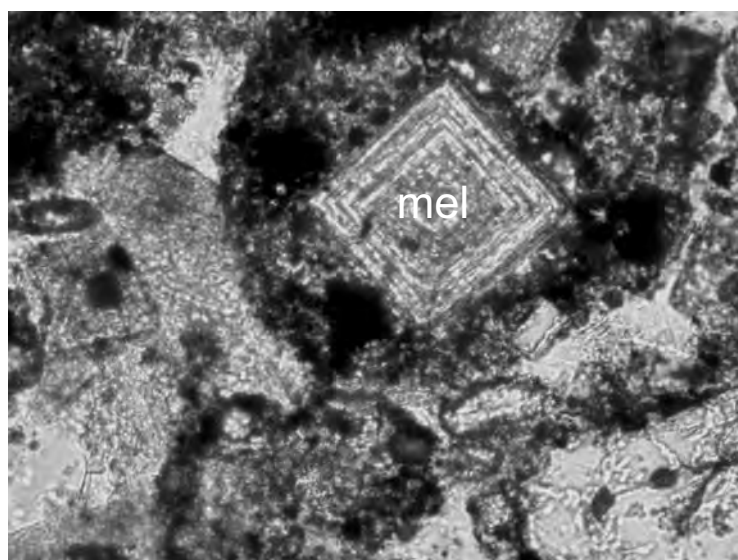


Figure 5



100μm

Figure 6

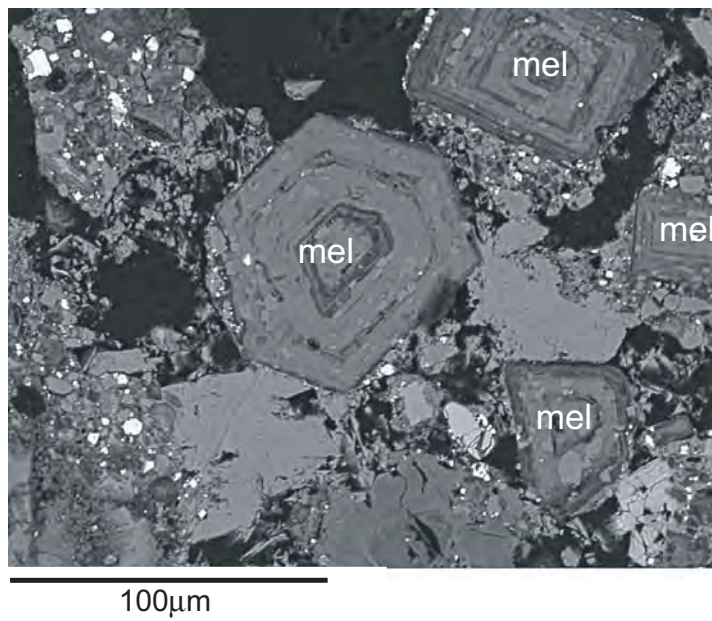
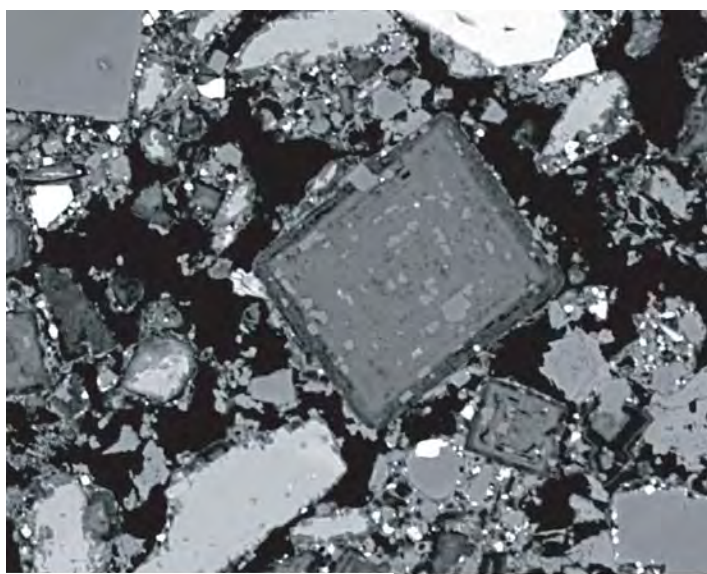


Figure 7





100µm

Figure 8

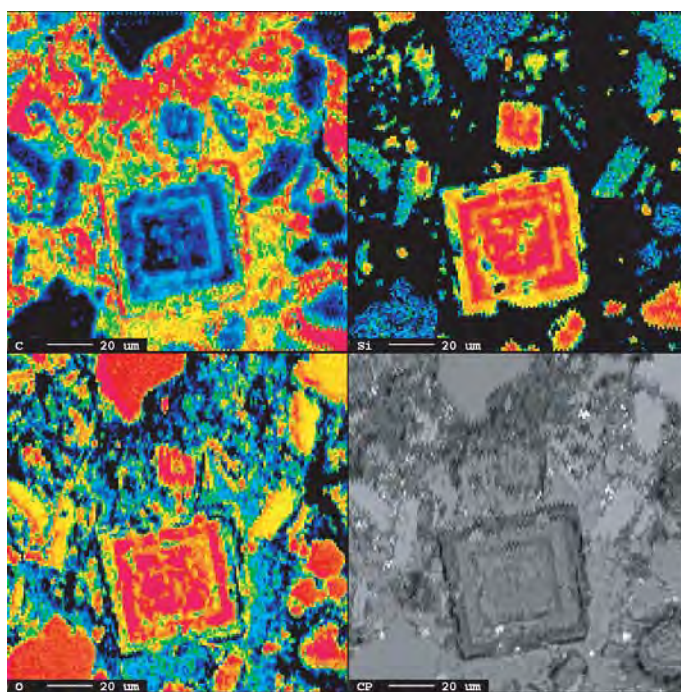


Figure 9

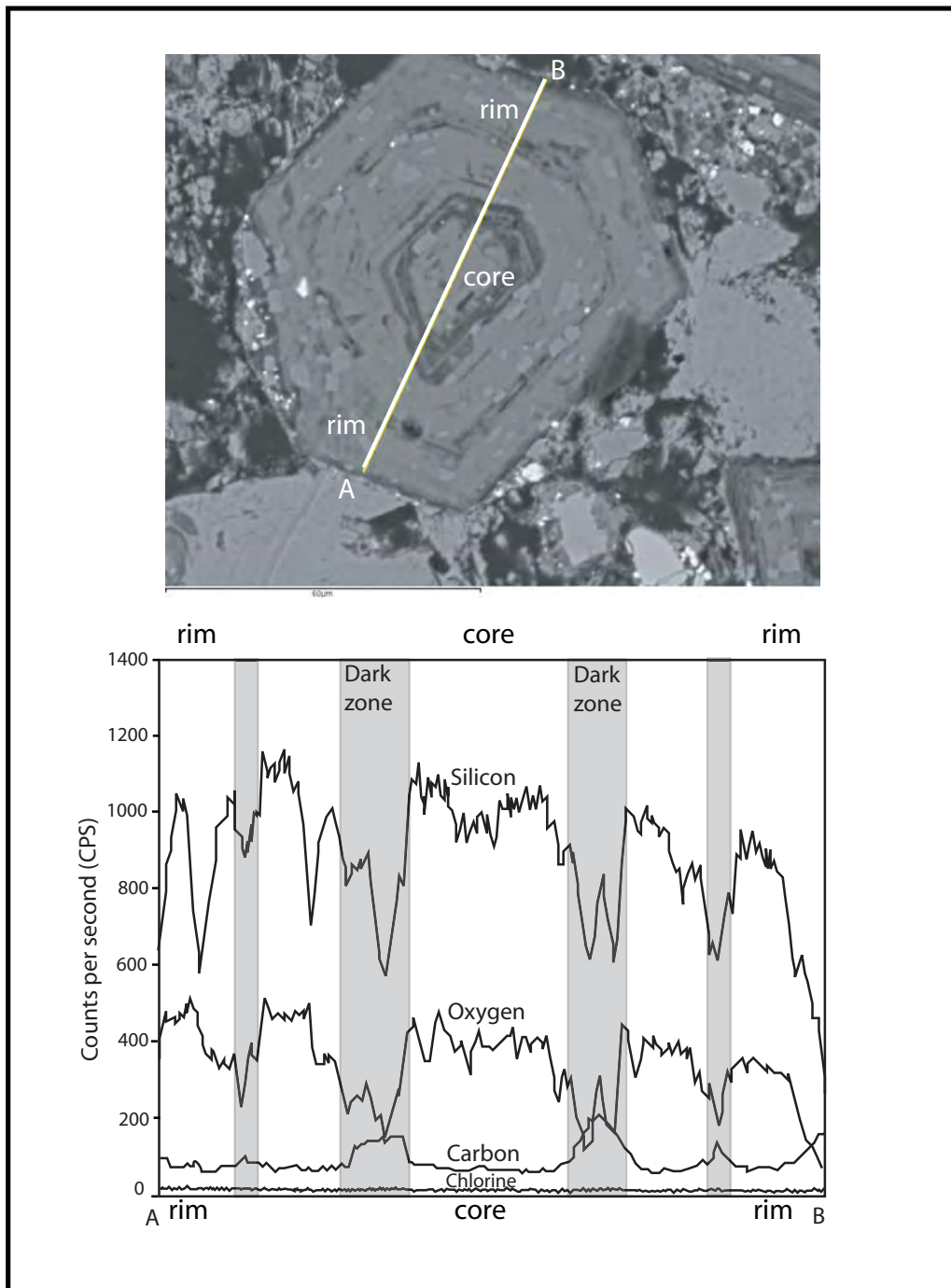


Figure 10